2024 European Control Conference (ECC)
June 25-28, 2024. Stockholm, Sweden

Dynamical system approach to navigation around obstacles

Aradhana Nayak[1] and Aude Billard [1]

Abstract— **In this article, we propose a dynamical system to avoid obstacles which are star shaped and simultaneously converge to a goal. The convergence is almost-global in a domain and the stationary points are identified explicitly. Our approach is based on the idea that an ideal vector field which avoids the obstacle traverses its boundary up to when a clear path to the goal is available. We show the existence of this clear path through a set connecting the boundary of the obstacle and the goal. The traversing vector field is determined for an arbitrary obstacle (described by a set of points) by separating it into cluster of stars. We propose an algorithm which is linear in number of points inside the obstacle. We verify the theoretical results presented with various hand drawn obstacle sets. Our methodology is also extended to obstacles which are not star-shaped, and, those which exist in high dimensions.**

I. Introduction

Dynamical systems (DS) remove the need of re-planning trajectories for obstacle avoidance in the presence of environmentally or artificially induced disturbances. This offers significant advantages over the online path planning algorithms such as Rapidly-exploring Random Tree (RRT, [1]) which rely on re-computation of a new path under a change in the scenario. Model-based optimization for path planning chooses from a set of trajectories satisfying the configuration space and robot constraints. It is hence suitable for situations where the robot dynamics is uncertain and has to be incorporated into the path planning. Notably, the Dynamic Window approach ([2], [3]) and the Curvature-Velocity Method ([4]) look for translational and rotational velocities that are achievable by the robot. Recently Model Predictive Control (MPC) has been also deployed in dynamic environments for real time goal reaching tasks ([5], [6], [7]). These methods leverage the high computation speed offered by modern computers to solve the optimal control problem in real time. Nonetheless they are subject to unknown local minima and hence do not guarantee global convergence to the goal position. Recently a method based on control Lyapunov barrier functions was proposed in [8] for simultaneous stabilization and goal convergence. However, as shown in [9] such functions do not exist.

One of the earliest DS based path planning approaches developed by Rimon and Koditschek in [10] utilizes artificial potential fields to navigate around obstacles ignoring the robot dynamics. It has a measure zero set of local maxima and, compared to the optimisation based approaches, it allows the robot to navigate at faster speeds without colliding with obstacles. The approach relies on analytical construction of diffeomorphisms to transform the configuration space into a simpler space. In [10] analytical diffeomorphisms are provided to transform the space of star shaped obstacles (star world) into a space of spheres (sphere world). Furthermore, it has been shown in [11] that there exists an analytical construction to determine the diffeomorphism transforming any surface which is homotopic to the sphere (generalized sphere) into a sphere in the same dimension.

[12] proposes navigating in a star world by considering a transformation into a point world. Special potential functions called navigation functions are known to exist which have a unique minimum and a measure zero set of maxima on a punctured disc in 2 dimensions and to a sphere punctured by spheres in higher dimensions. The pull back of the navigation function on the sphere world is a navigation function on the star world. Therefore, the integral curves of the negative gradient vector field of this navigation function converge almost globally to the unique minimum on the star world. These ideas have been extended to moving obstacles in [13] and to time varying goal positions in [14]. A DS converging to a goal is modified through a modulation matrix to avoid convex obstacles [15] and star shaped obstacles [16] which guarantees convergence to the goal position. Despite the analytical guarantees, it is challenging to construct a navigation function for an arbitrary obstacle which is not necessarily star shaped even in 2 dimensions as it requires a particular tree of stars structure as described in [11].

Our approach to navigation around the obstacle is briefly stated is as follows: (i) move along a level curve describing the obstacle until an 'escape set' is reached, (ii) switch by using bump functions to a linear goal oriented vector field in the escape set. We are hence assured not to be trapped in local minima and are free to use any vector field which does not penetrate the obstacle such as that proposed in [17]. It hence generalizes to star shaped obstacles in high dimensions and guarantees global asymptotic convergence to a desired goal position. We provide a clustering algorithm to segregate

[1]The authors are with the Learning algorithms and systems laboratory (LASA), Ecole Polytechnique Federale de Lausanne (EPFL), Switzerland aradhana.nayak@epfl.ch, aude.billard@epfl.ch

an arbitrary obstacle in 2 dimensions into star clusters and a navigation-like vector field to circumvent it. The algorithm complexity is of order $\mathcal{O}(DNK)$, where D is the dimension, N is the number of points describing the obstacle and K is the number of clusters. This enables construction of the dynamical system in real time when a closed form level set description of the obstacle is usually not available.

Our method of switching to the goal oriented vector field is inspired from [18] and [17] wherein a mixture vector fields is utilized for navigation and simultaneous path following and navigation respectively. Contrary to [17], where path following is the main objective, our aim is global convergence to a desired goal location while avoiding obstacles. Singular points arise frequently in regions where vector fields are added as shown in [17]. We provide an analysis which rules out the existence of singular points in any defined mixing region and by showing the existence of the escape set for an arbitrary obstacle.

The paper is organized as follows. In Section 2. we describe the methodology for multiple star shaped obstacles. In Section 3. we extend the proposed method for a tree of stars obstacle in $2D$. In Section 4. we consider an arbitrary obstacle in high dimensions. We present numerical experiments in Section 5. and conclude the paper in Section 6.

II. Star-Shaped Obstacle

In this section we construct a dynamical system which achieves almost global convergence to a desired goal point in $\mathbb{R}^n$ while avoiding a star-shaped obstacle.

Definition 1: A set $\mathcal{S} \subset \mathbb{R}^n$ is said to be star-shaped with respect to a point $c \in \mathcal{S}$ if for every $x \in \mathcal{S}$ the line segment from c to x is completely contained in $\mathcal{S}$. Additionally, it can be represented as a level set $\mathcal{S} = \{x \in \mathbb{R}^n : \phi(x) \leq 0\}$, $\phi : \mathbb{R}^n \to \mathbb{R}$ is a real valued analytical function with 0 being a regular value and, $\phi(c) < 0$. The boundary of $\mathcal{S}$ is denoted as $\mathcal{B}_\mathcal{S}$ and defined as $\mathcal{B}_\mathcal{S} \coloneqq \{x \in \mathbb{R}^n : \phi(x) = 0\}$.

Remark 1: Our definition of star-shaped set is referred to as *strictly star shaped* in [11].

Definition 2: The set $\mathcal{S}'$ is said to be a cover of a star-shaped set $\mathcal{S}$ with respect to c and defined as

$$\begin{aligned}\mathcal{S}' =&\{x \in \mathbb{R}^n : \|x - c\| \leq \|v\|\},\ v \coloneqq c - x_{max},\\ &x_{max} \in \{\max_{x \in \mathcal{S}} \|x - c\|\}\end{aligned}$$

The boundary of $\mathcal{S}'$ is denoted by $\mathcal{B}_{\mathcal{S}'} \coloneqq \{x \in \mathbb{R}^n : \|x - c\| = \|v\|\}$

Assumption 1: We assume that there are no critical points in the set $\phi^{-1}([0, d])$ for some $d > 0$. From Theorem 3.1 in [19], $\phi^{-1}(p)$ is diffeomorphic to, and a deformation retract of $\mathcal{B}_\mathcal{S}$ for all $p \in [0, \phi(x_{max})]$. The existence of $d > 0$ is shown in Theorem 3.2 in [19].

Lemma 1: ([11]) There exists a diffeomorphism $g : \mathcal{B}_\mathcal{S} \to \mathcal{B}_{\mathcal{S}'}$ defined as:

$$g(x) = c + \|v\| \frac{(x - c)}{\|x - c\|} \tag{1}$$

The following lemma shows that the normal to boundary of $\mathcal{S}$ at any point is never anti co-linear to the normal at the corresponding point on the boundary of the cover $\mathcal{S}'$.

Lemma 2: ([11]) Consider $y \in \mathcal{B}_{\mathcal{S}'}$ defined as $y \coloneqq g(x_1)$ for $g : \mathcal{B}_\mathcal{S} \to \mathcal{B}_{\mathcal{S}'}$ is defined in (1) and for $x_1 \in \mathcal{B}_\mathcal{S}$. Then we have,

$$\left.\frac{\partial \phi}{\partial x}\right|_{x = x_1} \neq c - y$$

In 2 dimensions, Lemma 2 guarantees us that adding the vector field which moves along the obstacle does not cancel out the vector field moving along its cover provided that the direction of traversal is preserved. However, for higher dimensions an analysis on the tangent space is necessary. In the following Lemma we examine the eigenvalues and vectors of the matrix $\left.\frac{\partial g^{-1}}{\partial y}\right|_{y = g(x)}$ at a point on the boundary $y \in \mathcal{B}_\mathcal{S}$, $y = g(x)$. The inverse $g^{-1}(y) \coloneqq c + \beta(y)(y - c)$ for some $\beta \in (0, \infty) : \phi(c + \beta(y)(y - c)) = 0$.

Lemma 3: Let the tangent space of $\mathcal{B}_{\mathcal{S}'}$ at y denoted by $T_y\mathcal{B}_{\mathcal{S}'}$ be comprised of the basis vectors $\{v_i\}_{i=1}^{n-1}$. Then, the eigenvalues of $\left.\frac{\partial g^{-1}}{\partial y}\right|_{y = g(x)}$ are $\underbrace{\beta(y), \ldots, \beta(y)}_{(n-1)\text{times}}, \beta(y) + (y - c)^\top \frac{\partial \beta}{\partial y}$. The corresponding eigenvectors are $\{v_i\}_{i=1}^{n-1}$ and $\frac{\partial \beta}{\partial y}$.

Proof: In Appendix A ■

We first consider the problem of avoiding a star shaped obstacle from almost all points in $\mathbb{R}^2$ and define the following vector fields:

$$\chi_1^+(x) \coloneqq R^+ \frac{\partial \phi}{\partial x}, \quad \chi_2^+(x) \coloneqq R^+(g(x) - c) \tag{2}$$

The matrix R^+ is the clockwise 90° rotation operator about the tangent plane. The tangent plane is that of the obstacle $\mathcal{B}_\mathcal{S}$ for χ_1^+ and of $\mathcal{B}_{\mathcal{S}'}$ for χ_2^+. We also define the vector fields denoted as χ_i^-, $i = 1, 2$ corresponding to counterclockwise rotation by 90° about the tangent

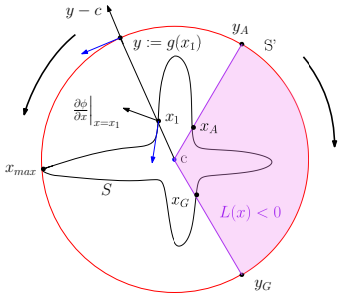

Fig. 1: Bi-directional vector fields

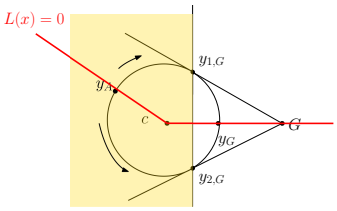

Fig. 2: y_A is chosen in the yellow region

planes of $\mathcal{B}_{\mathcal{S}}$ and $\mathcal{B}_{\mathcal{S}'}$ respectively as:

$$\chi_1^-(x) \coloneqq R^- \frac{\partial \phi}{\partial x}, \quad \chi_2^-(x) \coloneqq R^-(g(x) - c) \tag{3}$$

In 2 dimensions, we define the boundary function $L : \mathbb{R}^2 \to \mathbb{R}$ and the boundary set $\mathcal{B}_L \coloneqq \{x : L(x) = 0\}$ implicitly as a closed curve composed of three parts: the two line segments (i) joining the entry point $y_A \in \mathcal{B}_{\mathcal{S}'}$ to center c and (ii) center c to the exit point y_G and the last one, (iii) the shortest path in $\mathcal{B}_{\mathcal{S}'}$ connecting y_A and y_G. The points inside the set are shaded in pink and visualized in Figure 1. The vector field moving along the obstacle is defined as:

$$\chi_1(x) = \begin{cases} \gamma(x, x_G)\chi_1^+(x) & L(x) < 0 \\ \gamma(x, x_G)\chi_1^-(x) & L(x) > 0 \\ 0 & L(x) = 0 \end{cases}, \tag{4}$$
$$\gamma(x, x_G) \coloneqq e^{1-\epsilon_1/[\epsilon_1 - (x_G - x)^2]}$$

The parameter $\epsilon_1 > 0$ is defined to be small such that the ball $\{x : \|x - x_G\|^2 < \epsilon_1\}$ intersects $\mathcal{B}_{\mathcal{S}}$ at 2 points only. The scaling function γ ensures the convergence of the dynamical system $\dot{x} = \chi(x)$ to line joining x_G and y_G, all point on which are stationary points. The boundary $\mathcal{B}_L$ separates both $\mathcal{S}$ and $\mathcal{S}'$ into two distinct parts so that (4) is well defined. We define the following points formally (and refer the reader to Figure 1):

Definition 3: Given a goal G, an obstacle $\mathcal{S}$, its cover $\mathcal{S}'$ (in Definition 2), and a point $x_A \in \mathcal{B}_{\mathcal{S}}$:

1) $y_A \coloneqq g(x_A)$, $y_G \coloneqq g(x_G)$
2) $x_G \in \mathcal{B}_{\mathcal{S}}$ is the intersection of the line joining c and G with $\mathcal{B}_{\mathcal{S}}$

Next, we define a global vector field χ_2 traversing $\mathcal{B}_{\mathcal{S}'}$ similarly as:

$$\chi_2(x) = \begin{cases} \gamma(x, y_G)\chi_2^+(x) & L(x) < 0 \\ \gamma(x, y_G)\chi_2^-(x) & L(x) > 0 \\ 0 & L(x) = 0 \end{cases}, \tag{5}$$
$$\gamma(x, y_A) \coloneqq e^{1-\epsilon_2/[\epsilon_2 - (y_A - x)^2]}$$

The parameter $\epsilon_2 > 0$ is defined to be small such that the ball $\{x : \|x - x_G\|^2 < \epsilon_2\}$ intersects $\mathcal{B}_{\mathcal{S}'}$ at 2 points only. Note that the unstable points of χ_2 consist of the line joining x_A and y_A. Lastly we define a third dynamical system $\dot{x} = \chi_3$ which converges to the goal G globally and asymptotically:

$$\dot{x} = \chi_3(x) = G - x \tag{6}$$

χ_2 and χ_3 do not cancel each other when y_A is chosen in a specific region. As illustrated in Figure 2, y_A has to be chosen in the yellow region. Observe that if y_A is outside the yellow region, the vector fields χ_2 and χ_3 cancel at one of the points $y_{1,G}$ or $y_{2,G}$.

We have defined the three vector fields χ_i, $i = 1, 2, 3$ in (4)-(6). Before we start combining the vector fields, we will define regions where they do not mutually cancel each other. We first show that there exists a neighborhood around the point x_G where χ_1 and χ_3 do not cancel each other. More precisely we show that at x_G, the vector field $\chi_3(x_G) = G - x_G$ always has a component along the normal $\frac{\partial \phi}{\partial x}\Big|_{x=x_G}$.

Lemma 4: There exists a neighborhood $\mathcal{N}_{x_G}$ of x_G and a set $\bar{\mathcal{N}}_{x_G}$ defined as

$$\bar{\mathcal{N}}_{x_G} \coloneqq \{x + \alpha(G - x_G) : x \in \mathcal{N}_{x_G} \cap \mathcal{B}_{\mathcal{S}}\}, \alpha \in [0, 1] \tag{7}$$

such that

$$\left\langle G - z, \frac{\partial \phi}{\partial x} \right\rangle \neq 0, \ \forall z \in \bar{\mathcal{N}}_{x_G}. \tag{8}$$

Furthermore, the set $\bar{\mathcal{N}}_{x_G}$ can be expressed as

$$\bar{\mathcal{N}}_{x_G} = \{x : h(x) \leq \delta\} \tag{9}$$

for some $\delta > 0$ and for $h(x)$ which is defined as

$$h(x) = \sqrt{\|x - G\|^2 - \frac{\langle x - G, x_G - G\rangle^2}{\|x_G - G\|^2}}. \tag{10}$$

Proof: In Appendix B. The set $\bar{\mathcal{N}}_{x_G}$ is illustrated in pink in Figure 3. It is the tube shaped escape set from which G is 'directly' accessible. ■

Remark 2: Note that the set $\bar{\mathcal{N}}_{x_G}$ exists for an arbitrary obstacle $\mathcal{S}$ as well. In this case c is the center of the star

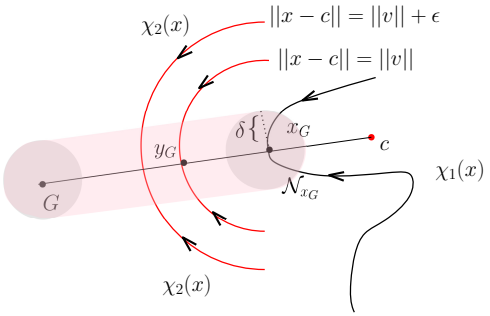

Fig. 3: $\mathcal{N}_{x_G}$ is a neighborhood of x_G where (21) holds, marked in grey. $\bar{\mathcal{N}}_{x_G}$ is the pink region which is a δ wide tube around the line joining G and x_G

cluster to which x_G belongs. For a given G, $x_G \in \mathcal{B}_{\mathcal{S}}$ is defined as $x_G = \arg\min_{x \in \mathcal{B}_{\mathcal{S}'}} \|x - G\|$ subject to the constraint that the straight line joining c, x_G and G does not intersect $\mathcal{S}$. In this case, there does not exist a single spherical cover so y_A is not defined. This however does not influence the statement of Lemma 4.

We also define three regions for corresponding to a small ϵ as follows:

$$\mathcal{R}_1 := \{x : \|x - c\| > \|v\| + \epsilon\} \tag{11}$$
$$\mathcal{R}_2 := \{x : \|v\| < \|x - c\| \leq \|v\| + \epsilon\} \tag{12}$$
$$\mathcal{R}_3 := \{x : \|x - c\| < \|v\|\} \tag{13}$$

Theorem 1: Assume a goal position G, a star-shaped obstacle obstacle $\mathcal{S}$ such that $\|G - c\| > \|v\| + \epsilon$ for some $\epsilon > 0$ and v defined in Definition 2. The dynamical system $\dot{x} = \chi(x)$ asymptotically converges to a goal G from all points other than the line joining x_A and y_A and, it is defined as:

$$\chi(x) = \sum_{i=1}^{4} \gamma_i(x)\chi_i(x) \tag{14}$$

where for $l_1 > 0$, and for $\epsilon < \|G - c\| - \|v\|$, the scaling functions γ_i, $i = 1, 2, 3, 4$ are:

$$\gamma_1(x) := \begin{cases} e^{l_1/(\|x-c\|-\|v\|-\epsilon)}, & \|x - c\| \leq \|v\| + \epsilon \\ 0, & \|x - c\| > \|v\| + \epsilon \end{cases}$$

$$\gamma_2(x) := \begin{cases} 0, & \|x - c\| < \|v\| \\ e^{l_1/(\|v\|-\|x-c\|)}, & \|x - c\| \geq \|v\| \end{cases}$$

$$\gamma_3(x) := \begin{cases} 0, & \|x - c\| < \|v\| + \epsilon \\ e^{l_1/(\|v\|+\epsilon-\|x-c\|)}, & \|x - c\| \geq \|v\| + \epsilon \end{cases}$$

$$\gamma_4(x) := \begin{cases} e^{l_1/(\delta - h(x))}, & h(x) \leq \delta \\ 0, & h(x) > \delta \end{cases},$$

with v defined in Definition 2, the function h defined in (10) and $\delta > 0$. The vector fields χ_1, χ_2 and χ_3 are defined in (4), (5) and (6) respectively.

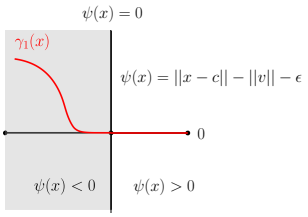

Fig. 4: Visualization of the mixing function γ_1

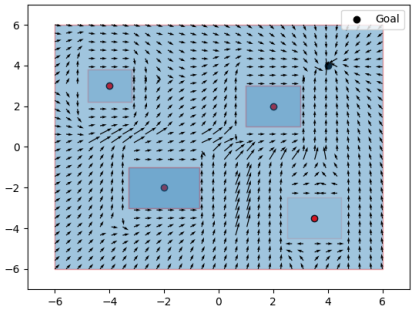

Fig. 5: Multiple star obstacles in $2D$ with $G = [4, 4]$

Proof: Let us consider each mixing region separately. In $\bar{\mathcal{N}}_{x_G}$, all the three vector fields χ_i, $i = 1, 2, 3$ are added. From Lemmas 2 and 4 we conclude the vector field does not vanish. In the region $\mathcal{R}_2$ the vector fields to be added are χ_1 and χ_2, which do not cancel out thanks to Lemma 2. In region $\mathcal{R}_1$, the vector fields to be added are χ_2 and χ_3 which also do not cancel out from Lemma 2. $\dot{x} = \chi(x)$ converges to G in the region $\mathcal{R}_1$ as the only active vector field in this region is χ_3. The dynamical system starting from all points outside the region $\mathcal{R}_1$ converges to the region $\bar{\mathcal{N}}_{x_G}$ by construction of χ_1 and χ_2. Further, the dynamical system starting from all points in $\bar{\mathcal{N}}_{x_G}$ converges to G as the active vector field in this region is χ_3.

■

Remark 3: The cover $\mathcal{S}'$ allows us to consider multiple star shaped obstacles in the configuration space. In case the sets $\bar{\mathcal{N}}_{x_G}$ intersect for multiple obstacles, we change the range of $\alpha \in (0, \alpha_{max})$ in (7) so that $x + \alpha_{max}(G - x_G)$ does not intersect any cover $\mathcal{S}'$ for any obstacle in the space. This is shown in Figure 5.

III. Tree of Stars Obstacle in 2 Dimensions

A spherical cover for a tree of stars is not well defined. However, the vector field χ_1 moving along the obstacle is well defined in 2 dimensions if the direction of rotation of normal is defined. In this section, we define the boundary set denoted by $\mathcal{B}_L$ for a tree of stars obstacle in $2D$ which is equivalent to (4) in the previous section.

It is a polygon which is obtained by traversing through star-shaped sets inside the obstacle. We decompose the arbitrary obstacle into star shaped sets in the following subsection.

A. Clustering into star shaped obstacles

Definition 4: A *tree of stars* set is a cluster of K star shaped obstacles. Each point in the set belongs to only one star shaped obstacle with a center $c_k, k \in 1, ..., K$.

Algorithm 1: To cluster set into tree of stars

Input : $\mathcal{S}$
Output: $\{\mathcal{S}_i, c_i\}_{i=1}^{K}$
1 Initialize $S_{out} = S$, $k = 1$;
2 **while** S_{out} *is nonempty* **do**
3 c_k= Random point in (S_{out}) ;
4 $S_k = \{x \in S_{out} : \alpha x + (1-\alpha)c_k \in S \; \forall \alpha \in (0,1)\}$;
5 $S_{out} = S \setminus \{\cup_{i=1}^{k} S_i\}$;
6 $k = k + 1$;
7 **end**

Any arbitrary obstacle can be clustered into a tree of stars set by the algorithm 1. The set minus operation in Line 5 of Algorithm 1 is maximum $\mathcal{O}(DN)$ for each iteration where D is the dimension of space, N is the number of points to be clustered. The complexity is therefore $\mathcal{O}(DNK)$, K being the number of clusters. The boundary set $\mathcal{B}_L$ is a closed polygon which is constructed as follows. Given any x_G, there are 3 possible choices for x_A as shown in Fig. 6 and denoted by x_A, ${x'}_A$ and ${x''}_A$. After a choice of x_A is made, we connect it with x_G through the centers and boundary points (denoted as b_{ij} in Figure 6) of connecting star subsets. The choice of b_{ij} is arbitrary. The sequence of subsets to be connected is obtained by generating a path in the tree graph connecting the star subset containing x_A with that the star subset containing x_G.

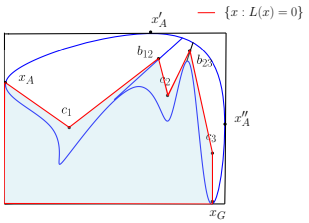

Fig. 6: $\{x : L(x) < 0\}$ is the light blue region. x_A may be chosen amongst x_G, ${x'}_A$ and ${x''}_A$, b_{ij} are boundary points for connected clusters i and j.

B. Obstacle avoidance for tree of stars obstacle

The vector field χ_1 is defined according to (4). We would like the obstacle avoiding dynamical system to:

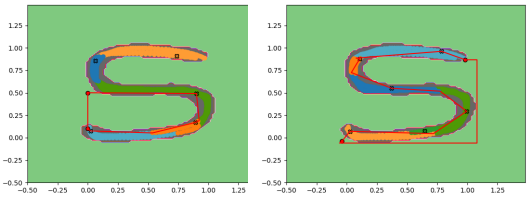

Fig. 7: Polygon $\mathcal{B}_L$ for arbitrary x_A with S shaped obstacle

(1) Follow the boundary of the obstacle using the vector field χ_1 defined in (4) , (2) Switch to χ_3 inside $\bar{\mathcal{N}}_{x_G}$. The result is stated in the following theorem.

Theorem 2: Consider an arbitrary obstacle $\mathcal{S}$ which is clustered in accordance with Algorithm 1, a goal point G outside $\mathcal{S}$, a neighborhood $\bar{\mathcal{N}}_{x_G}$ of G containing x_G and G as shown in Lemma 4 and the following vector field:

$$\chi(x) = \gamma_1(x)\chi_3(x) + \gamma_2(x)\chi_1(x) \tag{15}$$

where χ_1 is defined in (4) for the polygon boundary $\mathcal{B}_L$ and χ_3 is defined in (6). The mixing functions γ_1 and γ_2 are defined for $l_1 > 0$ as:

$$\gamma_1(x) := \begin{cases} 0, & h(x) < 0 \\ e^{-l_1/h(x)}, & h(x) \geq 0 \end{cases} \tag{16}$$
$$\gamma_2(x) := \begin{cases} e^{l_1/h(x)}, & h(x) \leq 0 \\ 0, & h(x) > 0 \end{cases}$$

Then, the dynamical system $\dot{x} = \chi(x)$ converges asymptotically to G from everywhere other than the edge of the polygon $\mathcal{B}_L$ containing x_A, and, outside $\mathcal{S}$.

Proof: The vector field $\dot{x} = \chi_1(x)$ converges to $\bar{\mathcal{N}}_G$ for all initial conditions outside it other than than the edge of the polygon $\mathcal{B}_L$ containing x_A, and, outside $\mathcal{S}$. All points in $\bar{\mathcal{N}}_G$ converge to G.

■

Remark 4: If Assumption 1 is not satisfied by the level set function ϕ defining $\mathcal{S}$, then, we restrict the domain of definition of the dynamical system to $\phi^{-1}[0, 0+\epsilon^*]$, where $\epsilon^* > 0$ is small enough so that $\phi^{-1}(\epsilon^*)$ is a deformation retract of $\mathcal{B}_{\mathcal{S}}$. The existence of ϵ^* is shown in Theorem 3.2 in [19].

IV. Single Obstacle in High Dimension

The vector fields in (4) are defined for a star shaped obstacle in $\mathbb{R}^2$. In this section we define a vector field on the star shape $\mathcal{S}$ induced by the vector field on the cover $\mathcal{S}'$ by a pull back through the diffeomorphism g as follows.

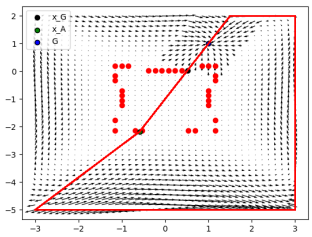

Fig. 8: Single star shape obstacle described by a level set. The points belonging to the set $\mathcal{B}_{\mathcal{S}}$ are marked with red dots. The edges of the polygon $\mathcal{B}_L$ are marked by red lines.

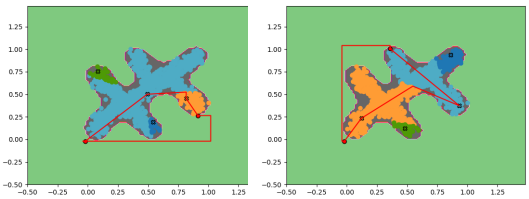

Fig. 9: Polygon $\mathcal{B}_L$ (in red) for an arbitrary hand drawn set. Note that different partitions of the same set can be obtained from Algorithm 1 as the choice of c_k is random.

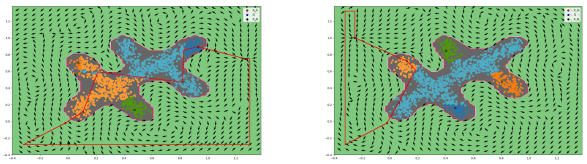

(a) $\dot{x} = \chi(x)$ converges to goal at $[1.25, 0.7]$ (b) $\dot{x} = \chi(x)$ converges to goal at $G = [-0.25, 1]$

Fig. 10: Avoiding obstacle in Figure 9

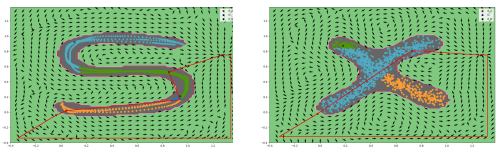

(a) $\dot{x} = \chi(x)$ converges to goal at $[1.25, 0.7]$ (b) $\dot{x} = \chi(x)$ converges to goal at $[1.25, 0.7]$

Fig. 11: Avoiding randomly hand-drawn obstacles

Definition 5: Consider a vector field $V : \mathcal{B}_{\mathcal{S}'} \to T\mathcal{B}_{\mathcal{S}'}$ defined on the manifold $\mathcal{B}_{\mathcal{S}'}$. Consider the diffeomorphism $g : \mathcal{B}_{\mathcal{S}} \to \mathcal{B}_{\mathcal{S}'}$ defined in (1). Then the vector field W induced on $\mathcal{B}_{\mathcal{S}}$ is defined as

$$W(x) \coloneqq \left.\frac{\partial g^{-1}}{\partial y}\right|_{y=g(x)} V(g(x)) \tag{17}$$

We now show that similar to Lemma 2 which holds for star shapes in 2 dimensions, that the vector field V on the $\mathcal{B}_{\mathcal{S}'}$ does not cancel out the one induced on $\mathcal{B}_{\mathcal{S}}$ if they are added together.

Lemma 5: Consider a point $x \in \mathcal{B}_{\mathcal{S}}$, any vector field V defined on $\mathcal{B}_{\mathcal{S}'}$ and the induced vector field W on $\mathcal{B}_{\mathcal{S}}$ as in Definition 5. The vector $V(g(x))$ satisfies

$$V(g(x)) \neq -\alpha W(x),\ \forall \alpha > 0,\ \forall x \in \mathcal{B}_{\mathcal{S}}. \tag{18}$$

Proof: In Appendix C ■

The vector field on $\mathcal{B}_{\mathcal{S}'}$ is defined as

$$V(y) = \sum_{i=1}^{n-1} \langle G - y, v_i \rangle\, v_i, \quad T_y\mathcal{B}_{\mathcal{S}'} = \{v_i\}_{i=1}^{n-1} \tag{19}$$

In the following Lemma we show that this vector field does not cancel out the vector field χ_3 defined in (6).

Lemma 6: Consider the vector field on $\mathcal{B}_{\mathcal{S}'}$ defined in (19). Then, for all $y \in \mathcal{B}_{\mathcal{S}'}$ we have

$$V(y) \neq -\chi_3(y) = -(G - y) \tag{20}$$

Proof: The vector $G - y$ belongs to the tangent subspace $T_y\mathcal{B}_{\mathcal{S}'}$ for all y in the set $\mathcal{S}$ defined as

$$\mathcal{S} = \{y \in \mathcal{B}_{\mathcal{S}'} : \langle G - y, y - c \rangle = 0\}$$

For the rest of the points $y \in \mathcal{B}_{\mathcal{S}'} \setminus \mathcal{S}$, (20) holds as $G - y$ does not belong to the subspace where $V(y)$ lives. Therefore we show that (20) holds for any $y \in \mathcal{S}$. For any such $y \in \mathcal{S}$, the vector field in (19) evaluates to $V(y) = G - y$. Therefore by definition, the inequality in (20) holds.

■

Theorem 3: Consider the goal point G, an obstacle $\mathcal{S}$, the potential function and vector field

$$V_f(y) = \frac{\langle y - y_A, y_G - y_A \rangle}{\|y_G - y_A\|},\ V(y) \coloneqq -\frac{\partial V_f}{\partial y},$$

for y_A and y_G defined in Definition 3. Consider vector field V on $\mathcal{B}_{\mathcal{S}'}$ is defined as $\chi_1 \coloneqq W(x)$ as defined in Definition 5 and, $\chi_2(y) \coloneqq V(y)$. Then the dynamical system $\dot{x} = \chi(x)$ with χ defined in (14) almost globally and asymptotically converges to G in a domain defined in Remark 4. The minima of the function V are unstable equilibrium points of the dynamical system.

Proof: By definition, $V(y)$ has unique minimum at y_G and maximum at y_A by definition. By Lemma 5,

the vector fields χ_1 and χ_2 do not cancel each other and, from Lemma 6, the vector fields χ_2 and χ_3 also do not cancel out. Further, from Lemma 4, the vector fields χ_1 and χ_3 do not cancel when they are mixed in the set $\bar{\mathcal{N}}_{x_G}$. Therefore, Theorem 1 holds for the vector fields χ_1, χ_2, χ_3 defined for high dimensional star-shaped obstacles. ■

Remark 5: The vector field χ_1 is difficult to construct with navigation functions in real time and, for an arbitrary obstacle. As an alternative, χ_1 can be chosen as the guiding vector field which follows an arbitrary smooth path on the manifold which was proposed in [20]. We only require this path to contain the point x_G. Thereafter, thanks to Lemma 4, there exists a set $\bar{\mathcal{N}}_{x_G}$ from which the dynamical system escapes to the goal. Since the integral curves of the guiding vector field are periodic, we are guaranteed to reach $\bar{\mathcal{N}}_{x_G}$ asymptotically. In this case the set of local maxima (unstable points) of the dynamical system are at the edge of the tube set $\bar{\mathcal{N}}_{x_G}$.

V. Results

Theorem 1 was tested on multiple box obstacles in 2 dimensions. The box obstacles are uniquely defined by the position of their centers and extents. The goal is placed at $[4, 4]$ in an arena which is a box centered at 0 with extent 6 in both directions. The results are shown in Figure 5. Theorem 2 was implemented on a star shaped obstacle defined by the level set $\mathcal{S} = \{(x_1, x_2) \in \mathbb{R}^2 : 2x_1^4 + 2(x_2+1)^4 - 3{x_1}^2(x_2+1)^2 - 2 \leq 0\}$. The goal is $(1, 1)$ and the star is centered at $(0, -1)$. The results are shown in Figure 8. Theorem 2 was also tested for an arbitrary obstacle by specifying it as a dense point cloud in $2D$. The level set description of the boundary was learnt using support vector clustering with hyper-parameters chosen through grid search. Thereafter, Algorithm 1 was applied to obtain the separating polygon $\mathcal{B}_L$ and hence obtain the vector field χ_1. A hand drawn point cloud was clustered as shown in Figure 9, S shaped hand-drawn character set was clustered as shown in Figure 7. Both these obstacles were navigated with the dynamical system $\dot{x} = \chi(x)$ defined in Theorem 2 as shown in Figures 10 and Figure 11(a) respectively. A hand drawn horseshoe shaped point cloud was also considered as shown in Figure 11(b). Observe that no limit cycles exist in Figure 8 as a closed form expression of the level set available. Contrary to this, some limit cycles can be observed in the hand drawn point clouds in Figures 10, 11(a)-(b) due to approximation of the level set by support vector clustering. It is also observed that the level set obtained by clustering is accurate in a small region around the obstacle as pointed out in Remark 4.

VI. Conclusion

In this article, the problem of navigating around an obstacle to reach a desired goal point using a dynamical system is addressed. Two methods are proposed depending on the shape of the obstacle: star shaped or arbitrary. The former assures almost global convergence in high dimensions. It is is also extended to navigation around multiple star shaped obstacles. The vector field defining the dynamical system in both the methods relies on the existence of a safe set from which the goal point is directly accessible. Arbitrary obstacles in $2D$ are shown to be navigated around by the proposed dynamical system in a local neighborhood around the obstacle. As future work, the domain of convergence of arbitrary obstacles can be extended by obtaining a level set description using SVM which is also a diffeomorphic retraction in a larger interval.

References

[1] Steven M LaValle and James J Kuffner. Rapidly-exploring random trees: Progress and prospects: Steven m. lavalle, iowa state university, a james j. kuffner, jr., university of tokyo, tokyo, japan. *Algorithmic and computational robotics*, pages 303–307, 2001.

[2] Dieter Fox, Wolfram Burgard, and Sebastian Thrun. The dynamic window approach to collision avoidance. *IEEE Robotics & Automation Magazine*, 4(1):23–33, 1997.

[3] Oliver Brock and Oussama Khatib. High-speed navigation using the global dynamic window approach. In *Proceedings 1999 ieee international conference on robotics and automation (Cat. No. 99CH36288C)*, volume 1, pages 341–346. IEEE, 1999.

[4] Reid Simmons. The curvature-velocity method for local obstacle avoidance. In *Proceedings of IEEE international conference on robotics and automation*, volume 4, pages 3375–3382. IEEE, 1996.

[5] Yuval Tassa, Nicolas Mansard, and Emo Todorov. Control-limited differential dynamic programming. In *2014 IEEE International Conference on Robotics and Automation (ICRA)*, pages 1168–1175. IEEE, 2014.

[6] Grady Williams, Paul Drews, Brian Goldfain, James M Rehg, and Evangelos A Theodorou. Aggressive driving with model predictive path integral control. In *2016 IEEE International Conference on Robotics and Automation (ICRA)*, pages 1433–1440. IEEE, 2016.

[7] Björn Lindqvist, Sina Sharif Mansouri, Ali-akbar Agha-mohammadi, and George Nikolakopoulos. Nonlinear mpc for collision avoidance and control of uavs with dynamic obstacles. *IEEE robotics and automation letters*, 5(4):6001–6008, 2020.

[8] Muhammad Zakiyullah Romdlony and Bayu Jayawardhana. Stabilization with guaranteed safety using control lyapunov–barrier function. *Automatica*, 66:39–47, 2016.

[9] Philipp Braun and Christopher M Kellett. Comment on "stabilization with guaranteed safety using control lyapunov–barrier function". *Automatica*, 122:109225, 2020.

[10] Elon Rimon. *Exact robot navigation using artificial potential functions*. Yale University, 1990.

[11] Elon Rimon and Daniel E Koditschek. The construction of analytic diffeomorphisms for exact robot navigation on star worlds. *Transactions of the American Mathematical Society*, 327(1):71–116, 1991.

[12] Nicolas Constantinou and Savvas G Loizou. Robot navigation on star worlds using a single-step navigation transformation. In *2020 59th IEEE Conference on Decision and Control (CDC)*, pages 1537–1542. IEEE, 2020.

[13] Robert A Conn and Moshe Kam. Robot motion planning on n-dimensional star worlds among moving obstacles. *IEEE Transactions on Robotics and Automation*, 14(2):320–325, 1998.

[14] Caili Li and Herbert G Tanner. Navigation functions with time-varying destination manifolds in star worlds. *IEEE Transactions on Robotics*, 35(1):35–48, 2018.

[15] Seyed Mohammad Khansari-Zadeh and Aude Billard. A dynamical system approach to realtime obstacle avoidance. *Autonomous Robots*, 32:433–454, 2012.

[16] Lukas Huber, Aude Billard, and Jean-Jacques Slotine. Avoidance of convex and concave obstacles with convergence ensured through contraction. *IEEE Robotics and Automation Letters*, 4(2):1462–1469, 2019.

[17] Weijia Yao, Bohuan Lin, Brian DO Anderson, and Ming Cao. Guiding vector fields for following occluded paths. *IEEE Transactions on Automatic Control*, 67(8):4091–4106, 2022.

[18] Savvas G Loizou, Herbert G Tanner, Vijay Kumar, and Kostas J Kyriakopoulos. Closed loop navigation for mobile agents in dynamic environments. In *Proceedings 2003 IEEE/RSJ International Conference on Intelligent Robots and Systems (IROS 2003)(Cat. No. 03CH37453)*, volume 4, pages 3769–3774. IEEE, 2003.

[19] John Willard Milnor. *Morse theory*. Number 51. Princeton university press, 1963.

[20] Weijia Yao, Bohuan Lin, Brian DO Anderson, and Ming Cao. Topological analysis of vector-field guided path following on manifolds. *IEEE Transactions on Automatic Control*, 2022.

APPENDIX

A. Proof of Lemma 3

From definition,

$$g^{-1}(y) = c + \beta(y)(y-c),\ \beta(y) : \phi(c+\beta(y)(y-c)) = 0$$
$$\frac{\partial g^{-1}}{\partial y} = \frac{\partial \beta}{\partial y}(y-c)^\top + \beta(y) I$$

The function $\beta(y)$ is continuous in y and $\beta(y) \in (0,1)$ for any $y \in \mathcal{B}_{\mathcal{S}'}$. Therefore the eigenvalues of $\frac{\partial g^{-1}}{\partial y}$ are $\underbrace{\beta(y), \ldots, \beta(y)}_{(n-1)\text{times}}, \beta(y) + (y-c)^\top \frac{\partial \beta}{\partial y}$. Observe that the eigenvectors of $\frac{\partial g^{-1}}{\partial y}$ are the same as those of the matrix $\frac{\partial \beta}{\partial y}(y-c)^\top$. The eigenvector corresponding to eigenvalue $\beta(y) + (y-c)^\top \frac{\partial \beta}{\partial y}$ is $\frac{\partial \beta}{\partial y}$.

$\{v_i\}_{i=1}^{n-1}$ is the set of eigenvectors of $\frac{\partial g^{-1}}{\partial y}$ corresponding to eigenvalue $\beta(y)$ since

$$\frac{\partial g^{-1}}{\partial y} v_i = \frac{\partial \beta}{\partial y}(y-c)^\top v_i + \beta(y) v_i = \beta(y) v_i$$

and $(y-c)$ is normal to $\mathcal{B}_{\mathcal{S}'}$ at y.

B. Proof of Lemma 4

We first show that (8) holds for $x = x_G$. As $G - x_G$ is aligned with $x_G - c$ we show that

$$\left\langle x_G - c, \frac{\partial \phi}{\partial x} \right\rangle \neq 0 \tag{21}$$

Assume that the converse is true. Therefore, $x_G - c \in T_{x_G}\mathcal{B}_{\mathcal{S}}$. For any trajectory $x(t) \in \mathcal{B}_{\mathcal{S}}$, there exists a unique trajectory $y(t) \in \mathcal{B}_{\mathcal{S}'}$ and hence,

$$x(t) = g^{-1}(y(t)) \implies \dot{x}(t) = \frac{\partial g^{-1}}{\partial y}\dot{y}.$$

Therefore, the vector $x_G - c \in T_{x_G}\mathcal{B}_{\mathcal{S}}$ can be expressed in terms of a vector in $\sum_{i=1}^{n-1} \lambda_i v_i \in T_{g(x_G)}\mathcal{B}_{\mathcal{S}'}$. From Lemma 3 we have:

$$x_G - c = \sum_{i=1}^{n-1} \frac{\partial g^{-1}}{\partial y}\lambda_i v_i = \sum_{i=1}^{n-1} \beta(y)\lambda_i v_i$$
$$\implies \|x_G - c\|^2 = 0$$

as $\langle x_G - c, v_i \rangle = \langle g(x_G) - c, v_i \rangle = \langle y_G - c, v_i \rangle = 0$. We conclude that the assumption is not true and hence (21) holds. As $\frac{\partial \phi}{\partial x}$ is a continuous function of x, there exists a neighborhood $\mathcal{N}_{x_G}$ of x_G such that (21) holds for all $x \in \mathcal{N}_{x_G}$ along with:

$$\text{sign}\left\langle G - x, \frac{\partial \phi}{\partial x} \right\rangle = \text{sign}\left\langle G - x_G, \frac{\partial \phi}{\partial x} \right\rangle.$$

Consider $z \in \bar{\mathcal{N}}_{x_G}$ defined in the statement in (7). As z is a translation of x by a fixed vector, $\frac{\partial z}{\partial x} = I$ and we have:

$$\frac{\partial \phi}{\partial z} = \frac{\partial \phi}{\partial x}\frac{\partial x}{\partial z} = \frac{\partial \phi}{\partial x}.$$

Therefore, (21) holds for any $z \in \bar{\mathcal{N}}_{x_G}$ and,

$$\left\langle G - z, \frac{\partial \phi}{\partial z} \right\rangle = \left\langle G - x, \frac{\partial \phi}{\partial x} \right\rangle + \alpha \left\langle G - x_G, \frac{\partial \phi}{\partial x} \right\rangle \neq 0$$

as both terms have same sign and are nonzero. Without loss of generality, we assume that $\mathcal{N}_{x_G} := \{x : \|x - x_G\| \leq \delta\}$. Therefore, $\bar{\mathcal{N}}_{x_G} = \{x : h(x) \leq \delta\}$ where $h(x)$ is defined in (10).

C. Proof of Lemma 5

We show that the matrix $\frac{\partial g^{-1}}{\partial y}\Big|_{y=g(x)}$ does not have a negative eigenvalue. Consider any vector $V(y) \in T_y\mathcal{B}_{\mathcal{S}'}$. Expressed along basis vectors $\{v_i\}_{i=1}^{n-1}$ of $T_y\mathcal{B}_{\mathcal{S}'}$, $V(y) = \sum_{i=1}^{n-1} \lambda_i v_i$, where $\lambda_i \in \mathbb{R}$. Further from Lemma 3 as v_i is an eigenvector of $\frac{\partial g^{-1}}{\partial y}$ with eigenvalue $\beta(y)$, we have,

$$\frac{\partial g^{-1}}{\partial y} V(y) = \sum_{i=1}^{n-1} \lambda_i \frac{\partial g^{-1}}{\partial y} v_i = \sum_{i=1}^{n-1} \lambda_i \beta(y) v_i = \beta(y) V(y)$$

As $\beta(y) > 0$, we conclude (18) holds for any y and by invertibility of g for any $x \in \mathcal{B}_{\mathcal{S}}$.